Mushroom *Inonotus sanghuang* alleviates experimental pulmonary fibrosis: Implications for therapy of pulmonary fibrosis

Xing Su [a,b,1], Kun Liu [c,1], Yu Xie [a,d], Mengdi Zhang [a], Xiao Wu [a], Yijie Zhang [a,2], Junpeng Wang [a,*,2]

[a] *Institute of Infection and Immunity and Translational Medical Center, Huaihe Hospital of Henan University, Kaifeng, 475000, China* [b] *Department of Respiration, The First Affiliated Hospital of Henan University, Kaifeng, 475000, China*

[c] *College of Biology Science and Engineering, Hebei University of Economics and Business, Shijiazhuang, Hebei, 050061, China* [d] *School of Physical Education, Henan University, Kaifeng, 475000, China*

ARTICLEINFO

Keywords:
Inonotus sanghuang
Polyphenols
Pulmonary fibrosis
Epithelial-mesenchymal transition
TGF-β

ABSTRACT

Mushroom *Inonotus sanghuang* has been characterized as a traditional medicine in China and has pharmacological activities to treat inflammation, gastroenteric dysfunction, and cancer. Recently, we reported the impact of *Inonotus sanghuang* extract (ISE) from ethyl acetate fraction on bleomycin (BLM)-induced acute lung injury in mice. Here, we aimed to investigate ISE's impact on pulmonary fibrosis using *in vivo* and *in vitro* models and the underlying mechanisms. To evaluate pulmonary fibrosis, female C57BL/6 mice fed ISE (0% or 0.6% in diet) for 4 weeks were instilled intratracheally with BLM and then continued the same diet before the end of the experiment. A549 cells were used to evaluate the epithelial-mesenchymal transition (EMT). Feeding ISE improved BLM-treated mice's survival via decreasing lung infiltrating cells and fibrosis, followed by reducing hydroxyproline content, collagen deposition, and mesenchymal markers (α-SMA and vimentin) while increasing epithelial marker E-cadherin. ISE also suppressed the TGF-β expression, Smad2/3 phosphorylation, and EMT- related transcription factor Snail upon BLM instillation. *Iin vitro* study demonstrated that ISE inhibited TGF- β-induced EMT-like phenotype and cell behaviors, the expression of α-SMA and vimentin, and prevented E- cadherin reduction of A549 cells. Consistent with *in vivo* study, ISE abrogated p-Smad2/3, and Snail expression. Finally, the influence of ISE on EMT was not due to ISE toxicity. Our findings indicated that ISE effectively attenuated BLM-induced lung fibrosis. These ISE properties were thought to be involved in interfering TGF-β Smad2/3 phosphorylation, and EMT process, suggesting that the material has the potential health benefits to improve lung fibrosis.

1. Introduction

Idiopathic pulmonary fibrosis (IPF) is a devastating disease without a known etiology [1], characterized by excessive deposition of extracellular matrix (ECM) and alternate scar tissues in the lung architecture that results in the gradual decline of pulmonary function, progressive respiratory failure, and eventually death [2]. Evidence demonstrates high mortality rates of IPF with the median survival of 2–3 years since diagnosis [3,4]. Although the underlying mechanisms of IPF have not yet been elucidated in detail, the pathophysiology of IPF is believed to be the result of the abnormal fibroblastic response caused by repetitive injuries and ineffective repair of pulmonary epithelial cells. Cytokine TGF-β serves as an important growth factor to induce fibroblasts' activation to undergo a phenotypic transition of myofibroblasts, which are the main factors in lung pathogenesis fibrosis [5–8]. Accumulating evidence has demonstrated that TGF-β is a crucial mediator in fibrosis to induce epithelial-mesenchymal transition (EMT) in IPF and is mainly mediated by Smad2/3 activation. Currently, pirfenidone and nintedanib have been used as the anti-fibrotic drugs to treat IPF [9] via inhibiting the TGF-β pathway and tyrosine kinases, respectively [1]. Therefore, the inhibition of TGF-β-induced EMT is regarded as the most efficacious target to treat IPF.

Although the etiology of IPF is still unknown, environmental factors such as smoking, infection, and drugs are associated with an increased risk of developing IPF. Nutrients have received increasing attention due to their diverse biological activities, such as anti-inflammatory, anti- tumor, and immunological properties in the lung [10,11]. Phytochemicals derived from fruits and vegetables are regarded as health-promoting environmental factors, potentially impacting chronic diseases [12]. Mushroom *Inonotus Sanghuang* (*I. sanghuang*) Sheng H. Wu, T. Hatt. & Y. C. Dai is a kind of

Abbreviations: α-SMA, α-smooth muscle actin; BAL, bronchoalveolar lavage; CCK8, cell counting kit-8; BLM, bleomycin; DAPI, 4,6-diamidino-2-phenylindole; ECM, extracellular matrix; ELISA, enzyme-linked immunosorbent assay; EMT, epithelial-mesenchymal transition; FBS, fetal bovine serum; H&E, hematoxylin-eosin; IPF, idiopathic pulmonary fibrosis; ISE, *Inonotus sanghuang* polyphenol extract; PF, pulmonary fibrosis; SEM, standard error mean; TGF-β, transform growth factor-β.

* Corresponding author at: Institute of Infection and Immunity of Huaihe Hospital, Henan University, 115 Ximen Street, Kaifeng, 475000, China. *E-mail address:* jpwangchina@henu.edu.cn (J. Wang).

[1] XS and KL contributed equally.

[2] JW and YZ shared the senior author.

https://doi.org/10.1016/j.biopha.2020.110919
Received 3 May 2020; Received in revised form 20 October 2020; Accepted 20 October 2020
Available online 14 November 2020
0753-3322/© 2020 The Author(s). Published by Elsevier Masson SAS. This is an open access article under the CC BY-NC-ND license (http://creativecommons.org/licenses/by-nc-nd/4.0/).

traditional Chinese medicinal plant mainly distributed in China, Japan, Korea, and other Asian countries [13]. Mushroom *I. Sanghuang* can improve blood circulation, relieve stomachaches, and exert anti-inflammation, anti-tumor, and anti-diabetes properties [14–17]. Besides, mushroom *I. sanghuang* extract has been proved to have anti-oxidant, anti-inflammatory, and anti-microbial properties [18–20]. Our study recently demonstrated that dietary *I. sanghuang* extract of ethyl acetate fraction cannot wholly prevent/treat but could attenuate acute lung injury, which may be via suppressing the production of inflammatory mediators and altering oxidative/anti-oxidative balance in mice [21]. However, there are limited studies to further explored the anti-fibrotic properties of *I. sanghuang* extract.

In the present work, we utilized *in vivo* and *in vitro* models to explore whether wild *I. sanghuang* extract from ethyl acetate fraction had an anti-fibrotic effect through an impact on TGF-β activated phenotype (migration, invasion, fibrotic ECM accumulation, and modulation). Current data ultimately suggests that wild *I. sanghuang* or its extract may be of interest in the prevention/treatment of lung fibrosis.

2. Materials and methods

2.1. Preparation of I. sanghuang polyphenol extract

Wild *I. sanghuang* was obtained from the Aershan Region of Inner Mongolia (Inner Mongolia, China). The authentication of this mushroom was done by Professor Xiangmei Zhang and a voucher specimen (NoF121725) deposited in the College of Biology Science and Engineering of Hebei University of Economics and Business, Shijiazhuang, China. *I. sanghuang* polyphenol extract (ISE) of ethyl acetate fraction was prepared as previously described [19] and was stored at -20 °C until further use.

2.2. Dietary ISE supplementation

Female-specific pathogen-free C57BL/6 mice (6 to 8-week old, 18− 20 g) were purchased from Nanjing Biomedical Research Institute of Nanjing University (Nanjing, China). Mice were randomized by body weight into three groups: Control: mice were fed a regular diet for 4 wks and then was instilled intratracheally with saline; BLM: mice were fed the same regular diet for 4 wks and then instilled with bleomycin (BLM) (Hanhui Pharmaceutical Co., Ltd, Hangzhou, China) (2.5 mg/kg); BLM + ISE: mice were fed a mixed diet with 0.6% ISE (w/w) prepared following our previous study [21] for 4 wks and then challenged with BLM. After BLM instillation, mice from three groups continued to consume the same diet before the end of this experiment. Twenty-eight days post-instillation, mice were euthanized with CO_2, and the lung tissue was collected for further analysis. Survival was recorded daily after the BLM challenge. All experimental procedures were conducted following the Guide for the Care and Use of Laboratory Animals by the National Institute of Health (NIH publication #85-23, revised in 1985) and approved by the Institutional Animal Care and Use Committee of Huaihe Hospital at Henan University.

2.3. Histological analysis

The left lung was fixed in 4% paraformaldehyde for 24 h and then processed for paraffin embedding. The lung was stained with hematoxylin-eosin (H&E) to evaluate cell infiltration as previously described [21] and stained with Masson's trichrome to evaluate pulmonary fibrosis under a photomicroscope. The semi-quantitative grading system described by Ashcroft et al. [22] was used to individually assess the severity of interstitial fibrosis in each successive field and a pre-determined severity scale was used to assign a score between 0 and 8. The pulmonary fibrosis classification's main criteria included alveolar or bronchiolar wall fiber thickening, collagen deposition, infiltrating inflammatory cells, and edema. 0, normal lung; 1, minimal fibrous thickening of the alveolar or bronchiolar walls; 2–3, moderate thickening of the lung wall without significant damage to the lung structure; 4–5, fibrosis increased with definite damage to the lung structure and the formation of a fibrous band or small fibrous masses; 6–7, severely distorted structures and large areas of fibrous tissue as well as "honeycomb lung." severe distortion of the structure and large fibrous areas and "honeycomb lung" is placed in this category; 8, total fibrous visual field occlusion. *2.4. Hydroxyproline assay*

The supernatant from lung homogenates in mice right lung was prepared as previously described [21], and the hydroxyproline content was assessed using a hydroxyproline kit (Nanjing Jiancheng Bioengineering Institute, Nanjing, China) following the manufacturer's instructions. *2.5. Sircol assay*

Total soluble collagen in lung tissue was measured using the Sircol collagen assay (Biocolor Ltd, Belfast, UK) following the manufacturer's instructions. One milliliter of Sirius Red reagent was added to lung tissue was prepared as a homogenate and mixed. The collagen–dye complex was precipitated and separated by centrifugation and dissolved in an alkali reagent. Finally, the samples were loaded into a microplate reader and the absorbance was determined at 555 nm.

2.6. Analysis of inflammatory cells and TGF-β levels in bronchoalveolar lavage (BAL) fluid

On day 28 post-instillation with BLM, mice were euthanized with CO_2, and we collected the cell-free fluid of BAL and the BAL cells from the left lung described as previous [21]. We used the cell-free fluid of BAL to measure the TGF-β level using the Human/Mouse TGF-β1 ELISA kit (eBioscience, San Diego, CA, USA) following the manufacturer's instructions. We used the BAL cells to determine total inflammatory cells using trypan blue staining and cell compositions using flow cytometry as previously described [21].

2.7. Cell culture

A549 cells (human type II alveolar epithelial cells) were cultured in Dulbecco's Modified Eagle Media supplemented with 10% FBS and 1% penicillin/streptomycin in an incubator at 37℃ with

5% CO_2. The cells (2.5×10^5/well) were seeded in a 24-well plate. When the cells reached about 40–50% confluence, the medium was changed with serum-free DMEM and then cultured overnight. After the cells were treated with 0, 2, and 4 μg/mL ISE at the indicated time in the absence of TGF-β, we evaluated ISE's cytotoxicity by a colorimetric CCK8 assay kit (Dojindo, Kumamoto, Japan) following the manufacturer's recommendations. Besides, A549 cells were cultured with 0, 2, and 4 μg/mL ISE for 2 h and then were administrated with 5 ng/mL recombinant human TGF-β1 (Sino Biological Inc., Beijing) for 24 or 48 h. Finally, typical morphological changes in A549 cells were observed under a microscope, and the cells were collected to do further analysis. ISE doses used in this study were chosen according to our previous study [20].

2.8. Cell invasion assays

A549 cells were cultured into a 24-well plate to develop a confluent monolayer. When the cells reached about 80% confluence, the crossover was performed utilizing a 1000 μL sterile pipette tip. After the scratched cells were removed with sterile PBS, the cells were treated with 5 ng/mL TGF-β1 (Sino Biological, Inc., Beijing, China) for 24 h after pre-treated with 0, 2, and 4 μg/mL ISE for 2 h. A scratch-healing assay was performed using low serum (0.2% FBS) medium. On a phase contrast optical microscope, photographs are taken at 0 and 24 h utilizing positioning lines to ensure that the identical points are the same. The following formula calculated the invasion index:

invasion index (%) = [(the width of the initial scratch) − (the final width of the scratch)] / (the width of the initial scratch).

2.9. Migration assay

Matrigel (Invitrogen, CA, USA) was transferred from -20℃ to 4℃ for 12 h to obtain a liquid state for use. The upper chamber of the transwell's basement membrane (Corning, NY, USA) was coated mixture of matrigel and medium (the dilution ratio is 1:8) and dried at room temperature. The cells were trypsinized and seeded in the upper chamber (Corning, Corning, USA) with the serum-free medium at a density of 1×10^5 cells/well. DMEM containing 10% FBS was added to the lower chamber. After incubation at 37°C in a humid atmosphere for 24 h, non-migrating cells were removed with a swab, and migrating cells were fixed with 4% paraformaldehyde and stained with 0.1% crystal violet.

2.10. Immuno-fluorescence staining

After A549 cells were co-cultured with TGF-β1 for 24 h in combination with 0, 2, and 4 μg/mL ISE, they were washed, fixed, permeabilized with 0.1 % Triton X-100 in PBS, and blocked with 0.5 % FBS in PBS. The fixed/permeabilized cells were incubated with anti-Vimentin antibody overnight and then were stained with Alexa Fluor 488 conjugated secondary antibodies (Invitrogen) for 1.5 h. Cell nuclei were identified by 4,6-diamidino-2-phenylindole (DAPI) staining, and then the Vimentin expression was measured by immune-fluorescence microscopy.

2.11. Western blot

The right lung tissue and A549 cells were lysed in RIPA lysis buffer, and the supernatant was quantified using the BCA Protein Assay Kit, as previously described [21]. The supernatant was resolved on 7.5% acrylamide SDS-PAGE gels and transferred to nitrocellulose membranes. After blocked with 5% non-fat milk, the membrane was incubated with specific primary antibodies for the following proteins: Type I collagen (Col I) (1:1000) (Bioss, Beijing, China), α-Smooth muscle actin (α-SMA) (1:1000) (Sino Biological, Inc.), E-Cadherin (E-Cad) (1:1000), Vimentin (1:1000), Snail (1:1000), Smad2/3 (1:1000), phosphorylated Smad2/3 (p-Smad2/3) (1:1000) (all from Cell Signaling Technologies, Danvers, MA), and β-actin (1:5000) (Sigma-Aldrich) and then treated with horseradish peroxides (HRP)-conjugated secondary antibodies followed by exposure to enhanced chemiluminescent reagents (Millipore, Burlington, MA).

2.12. Statistical analysis

All statistical analysis was made using Prism 8.0 software (GraphPad). Kaplan-Meier survival analysis with log-rank test was employed to compare the difference in survival rates. One-way ANOVA, followed by Tukey's HSD *post-hoc* test for multiple comparisons, was performed. A statistically significant difference was defined as $p < 0.05$ compared with the indicated group.

3. Results

3.1. ISE alleviates BLM-induced lung fibrosis in mice

Following BLM's intratracheal instillation, BLM-treated mice's survival rate at 28 days was 66.7%, followed by the 25% increase in the BLM + ISE group's survival rate to the BLM group (Fig. 1A). Infiltrating inflammatory cell analysis in BAL (Fig. 1B) showed that BLM treatment increased the numbers of total infiltrating cells, macrophages, and neutrophils. Such a rise was reduced by ISE treatment, further demonstrated by lung histologic changes (Fig. 1D and F). However, BLM instillation resulted in an increased percentage of neutrophils, not macrophages, but this effect was not further affected by ISE (Fig. 1C).

To explore the effect of ISE on lung fibrosis, we evaluated the lung collagen deposition. Histologic analysis of lung tissue from these animals demonstrated that, compared to that of control, BLM dramatically increased collagen deposition (Fig. 1E and G), which was further confirmed by increased hydroxyproline content (Fig. 2A) and collage production (Fig. 2B and C), and such rise was reversed by ISE supplementation.

3.2. ISE suppresses BLM-induced EMT in mice

The EMT plays a crucial role in the pathogenesis of lung fibrosis. We explored ISE's effects on the protein level of EMT markers, including E- cadherin,

vimentin, and α-SMA in mice lung tissue specimens. As shown in Fig. 3, BLM administration in mice lung resulted in a significant decrease in E-cadherin expression and an increase in vimentin and α-SMA. However, ISE restored the expression of E-cadherin and decreased expression of vimentin and α-SMA. These data suggested that ISE might have the ability to attenuate BLM-induced lung fibrosis in mice by inhibiting the progress of EMT.

3.3. ISE reduces TGF-β-induced Smad2/3 phosphorylation and Snail in mice

TGF-β is an important pro-fibrotic mediator to induce EMT in the progression of lung fibrosis. Thus, we investigated whether the inhibitory effects of dietary ISE on lung fibrosis was due to its regulation of TGF-β levels in mice lung BAL. BLM instillation increased the concentrations of lung TGF-β. While ISE supplementation resulted in a significant reduction of TGF-β in BLM-induced mice (Fig. 4A). We subsequently measured whether ISE was involved in the downstream target genes of TGF-β. Smad2 and Smad3 are two critical downstream factors of TGF-β in lung fibroblasts, and we found that BLM notably increased Smad2/3 phosphorylation in an IPF model. However, ISE inhibited the increased level of p-Smad2/3 caused by BLM (Fig. 4B and D). Besides, the expression of Snail1, a transcriptional repressor and promoter of EMT [23], was up-regulated in the lung tissue after BLM challenge; while this effect was reversed with ISE supplementation (Fig. 4C and D).

3.4. ISE inhibits TGF-β-induced morphological changes in A549 cells

To explore whether ISE could influence the TGF-β-induced EMT process, we evaluated the cell morphology and EMT marker's expression in human A549 cells treated with different dose of ISE with/without

Fig. 2. ISE inhibits collagen deposition in mice pulmonary damage induced by BLM. Collagen deposition was measured quantitatively by assaying for hydroxyproline concentrations (A) and collagen production (B and C) from the right lung.

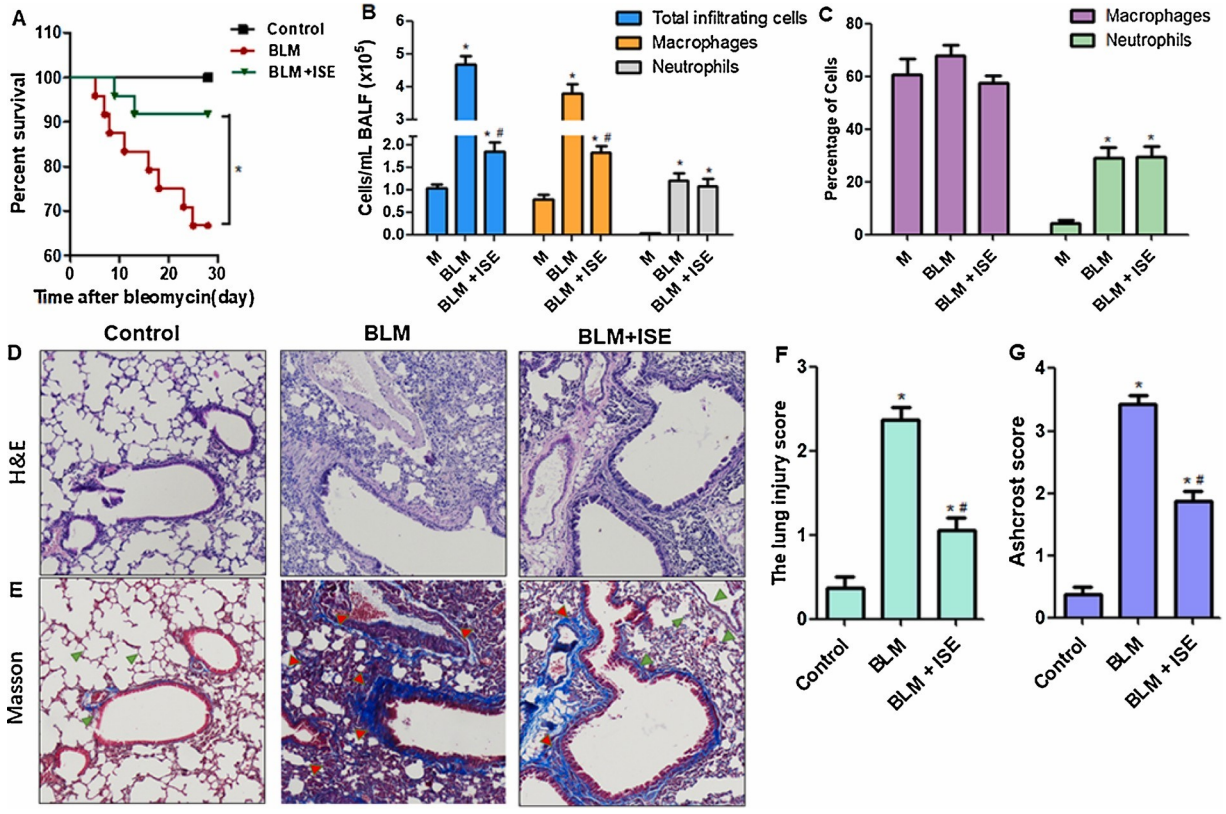

Fig. 1. ISE improves the survival and inhibits pulmonary inflammation and fibrosis on day 28 in mice pulmonary damage induced by BLM. The mortalities were recorded throughout the observation period upon BLM installation (A). Kaplan-Meier survival analysis with log-rank test was used to compare the survival rates among the three groups. *$p < 0.05$ vs. BLM. (B and C) The total infiltrating cells in the BAL were measured by trypan blue assay. The macrophages and neutrophils in the BAL were determined using the flow cytometry method. (D and E) Representative images from H&E and Masson's staining show lung infiltrating cells and fibrosis (magnification, × 100) on day 28 after the BLM challenge, respectively. (F and G) The lung injury score and Ashcroft score were used to evaluate lung cell infiltration and fibrotic lesions, respectively. Values are expressed as the mean ±SEM (n = 8-12 mice/group). Green arrows mean Ashcroft score 1-2; Red arrows mean Ashcroft score 4-5. *p < 0.05 vs. control; #$p < 0.05$ vs. BLM. ISE, *I. sanghuang* polyphenol extract; BLM, bleomycin.

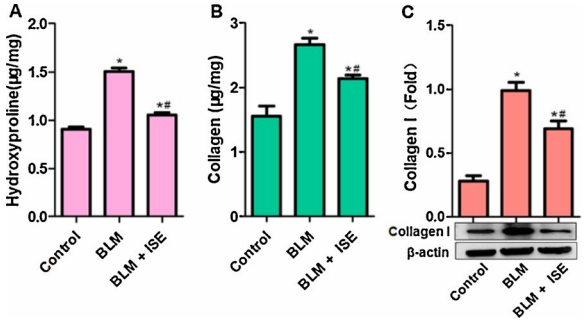

Collage I was normalized against β-actin. β-actin was used as a loading control. The control (BLM) value was set at 1, and the relative value was presented as fold induction of that of the control (BLM). Values are expressed as the mean ±SEM (n = 8-12 mice/group). *$p < 0.05$ vs. control; #$p < 0.05$ vs. BLM. ISE, *I. sanghuang* polyphenol extract; BLM, bleomycin.

TGF-β. As shown in Fig. 5A–D, ISE reversed alterations in cell morphology 48 h after TGF-β treatment. Subsequently, we accessed the influence of ISE on the A549 cellviability post-administration with ISE in the absence of TGF-β. The cell viability showed no difference with ISE at the indicated concentrations (Fig. 5E). These findings suggested that ISE might directly reverse TGF-β-induced EMT cell morphology that was not mediated by ISE's cytotoxicity.

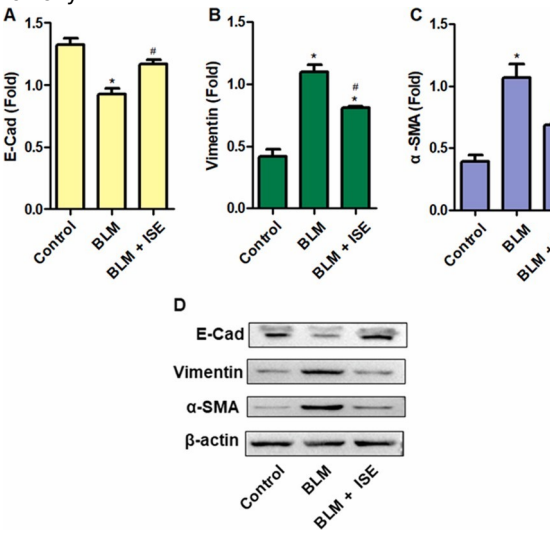

Fig. 3. ISE increases epithelial marker E-cadherin and decreases mesenchymal markers vimentin and α-SMA on day 28 in mice pulmonary damage induced by BLM. Western blot was applied to assess the change of expression of E-cadherin (A and D), vimentin (B and D), and α-SMA (C and D) for each group of mice. E- cadherin, vimentin, and α-SMA were normalized against β-actin. β-actin was used as a loading control. The control (BLM) value was set at 1, and the relative value was presented as fold induction of that of the control (BLM). Values are expressed as the mean ±SEM (n = 8-12 mice/group). *$p < 0.05$ vs. control; #$p < 0.05$ vs. BLM. ISE, *I. sanghuang* polyphenol extract; BLM, bleomycin.

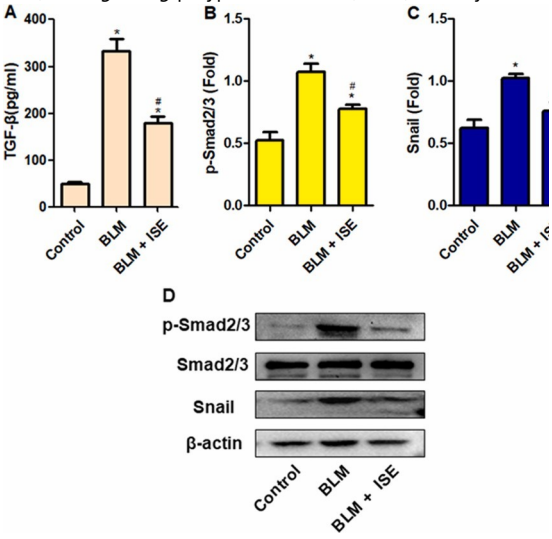

Fig. 4. ISE decreases the TGF-β1 levels of lung BAL fluid and inhibits the Smad2/3 phosphorylation and the expression of EMT-related transcription factor Snail1 on day 28 in mice. The levels of TGF-β (A) in the BAL fluid were measured using ELISA assay, and (B–D) the expression of phosphorylated Smad2/3 and Snail1 were determined by western blot assay in the lysates of lung tissues from each group of mice. p-Smad2/3 normalized against Smad2/3. Snail1 normalized against β-actin. β-actin was used as a loading control. The control (BLM) value was set at 1, and the relative value was presented as fold induction of that of the control (BLM). Values are expressed as the mean ±SEM (n =8-12 mice/group). *$p < 0.05$ vs. control; #$p < 0.05$ vs. BLM. ISE, *I. sanghuang* polyphenol extract; BLM, bleomycin.

3.5. ISE inhibits TGF-β-induced reduction EMT and collage I production in A549 cells

EMT process is always accompanied by reducing epithelial cell markers and increasing mesenchymal cell markers. Then, we evaluated the potential impact of ISE in pulmonary EMT markers. As shown in Fig. 6A–C, TGF-β1 treatment significantly reduced epithelial marker E- cadherin and increased mesenchymal markers vimentin and α-SMA, and such was restored by ISE. Data for expression of vimentin was further confirmed by immunofluorescent analysis (Fig. 6E). Collagen I, a fundamental component of the extracellular matrix, was measured by the Western blot assay. We found that ISE attenuated the TGF-β1- induced increase of Collagen I (Fig. 6D). Based on these results, these data suggested that ISE attenuated TGF-β1-induced pro-fibrotic effects through inhibition of EMT.

3.6. Anti-EMT effect of ISE is mediated by inhibition of Smad2/3 activation and Snail expression in A549 cells

Then, we determined whether ISE administration could impact the downstream signal (Smad2/3 activation) of TGF-β. Consistent with *in vivo* data, TGF-β treatment resulted in the Smad2/3 phosphorylation, and such rise was blunted by ISE (Fig. 7A).

Snail1, a critical transcription factor, can bind the E-cadherin promoter region to initiate EMT [23,24]. Thus, we also determined whether ISE affects the expression of EMT-related transcriptional factor Snail1. The expression of Snail was significantly increased by TGF-β, while ISE blocked TGF-β-induced Snail protein expression (Fig. 7B).

3.7. ISE prevents TGF-β-induced migration and invasion in A549 cells

To measure the inhibitory impact of ISE on TGF-β-induced EMT on cell migration and invasion, we performed healing and transwell assay, respectively. TGF-β-treated A549 cells displayed higher migration and invasion abilities, but ISE dose-dependently could inhibit TGF-β-induced cell migration and invasion (Fig. 8).

4. Discussion

IPF is characterized by cycles of lung tissue damage and repair [25]. TGF-β is regarded as the fibrogenic master regulator with multiple functions

on ECM turnover, epithelial cell differentiation, inflammation, immunosuppression, and cancerogenesis. In the lung, TGF-β levels are

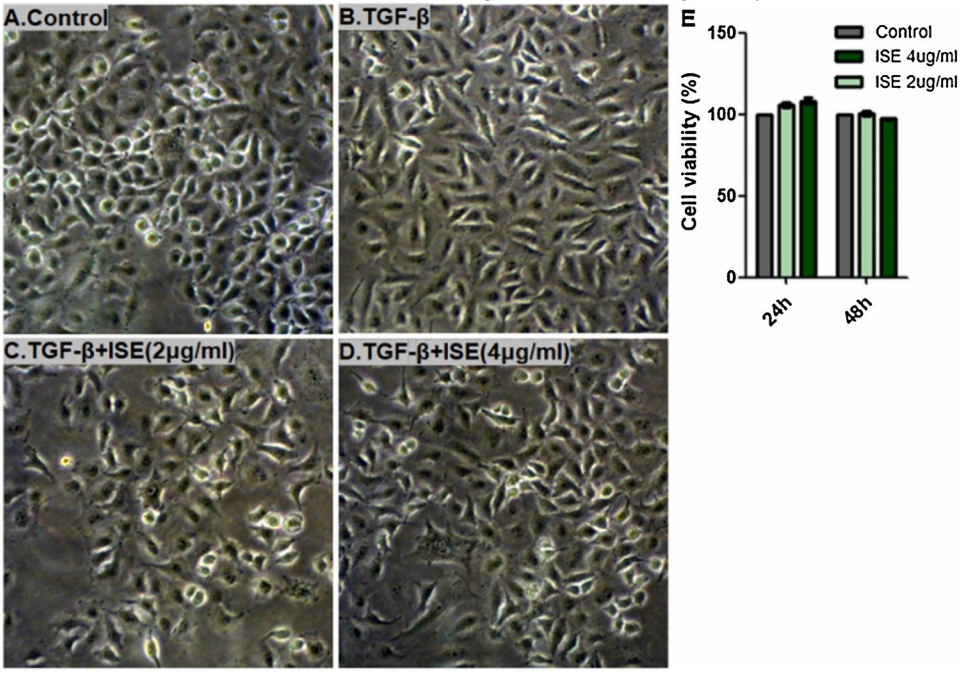

Fig. 5. Effect of ISE on the morphological changes and cell viability of TGF-β-treated A549 cells (magnification, 200 ×). (A–D) Pictures are representative images of the A549 cells per group 48 h after TGF-β administration. (E) A549 cells were treated with ISE at the indicated concentrations for 24 and 48 h, and then cell viability was determined by the CCK-8 assay. The summary values are expressed as the mean ±SEM of samples (n =3). ISE, *I. sanghuang* polyphenol extract.

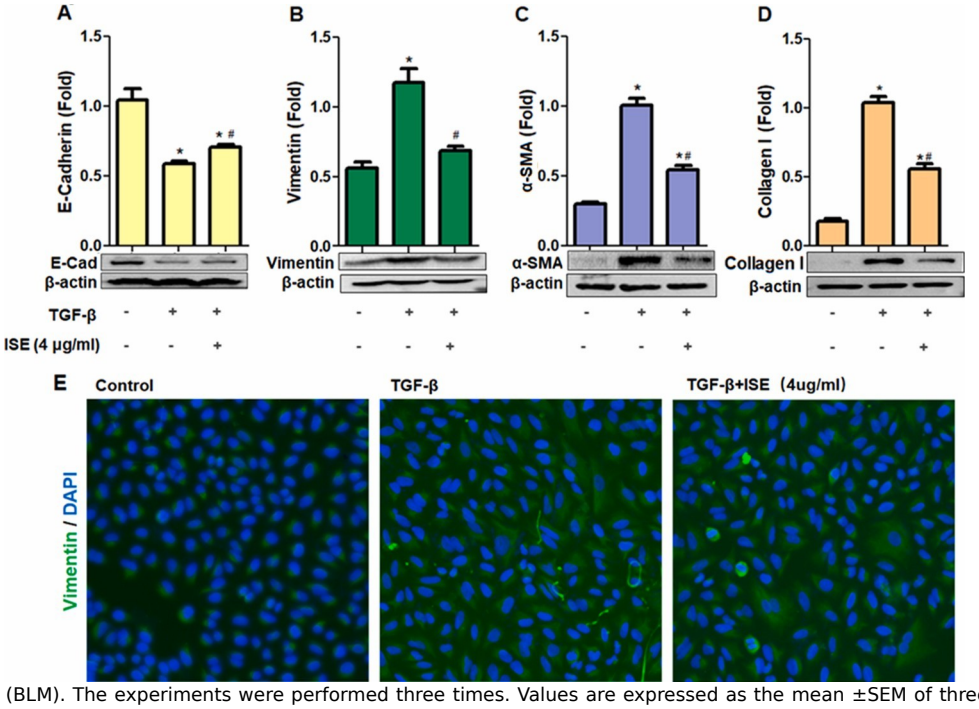

Fig. 6. ISE affects the expression of EMT-related markers in TGF-β-induced A549 cells. Expression of E-cadherin (A), vimentin (B), α-SMA (C), and collage 1 (D) in the lysates of A549 cells 48 h after under the indicated treatment were analyzed by Western blot assay. E-cadherin, vimentin, α-SMA, and collage I were normalized against β-actin. The experiments were performed three times. β-actin was used as a loading control. The control (BLM) value was set at 1, and the relative value was presented as fold induction of that of the control (BLM). The experiments were performed three times. Values are expressed as the mean ±SEM of three samples. $^{*}p < 0.05$ vs. control; $^{\#}p < 0.05$ vs. TGF-β. Furthermore, the expression of vimentin (E) was detected by immunofluorescence (200 ×). Green fluorescence indicates the mesenchymal marker vimentin. Cell nuclei are indicated in blue with DAPI. ISE, *I. sanghuang* polyphenol extract.

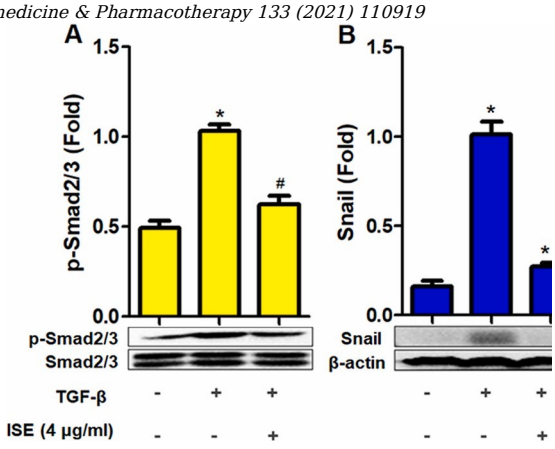

Fig. 7. ISE inhibits the Smad2/3 phosphorylation and the Snail1 expression in TGF-β-treated A549 cells. Western blot analysis of phosphorylated Smad2/3 (p- Smad2/3) (A) and Snail1 (B) expression in A549 cells 48 h after under the indicated treatment. The experiments were performed three times. β-actin was used as a loading control. The control (BLM) value was set at 1, and the relative value was presented as fold induction of that of the control (BLM). Values are expressed as the mean ±SEM of three samples. $^{*}p < 0.05$ vs. control; $^{\#}p < 0.05$ vs. TGF-β. ISE, *I. sanghuang* polyphenol extract.

evaluated in IPF patients and fibrotic animal models [25–30]; TGF-β is involved in all known myofibroblastic differentiation and activation pathways [25]. Therefore, it is undoubted that TGF-β is the most effective inducer of ECM synthesis, especially for collagen [27]. BLM is the most widely used agent for the induction of experimental pulmonary fibrosis, an irreversible change linked to tissue inflammation, as well as to the elevated TGF-β secreted by the bronchial epithelium [31]. In the present study, BLM induced the fibrotic changes and increased the TGF-β production of the lung in BLM-treated mice, but this was significantly attenuated in treatment with ISE supplementation.

Elevated TGF-β carries out its action via triggering complex intracellular signal pathways [32]. Following activation, TGF-β conjugates to its receptors and initiates a canonical and noncanonical signal pathway to promote fibrosis and modulates immune responses and inflammation [33,34]. After Smad2 and Smad3 proteins are activated via phosphorylated Smad2 and Smad3 in serine/threonine site, phosphorylated Smad2/3 forms complexes with Smad4 [35] and translocate into the nucleus, where they coordinate with sequence-specific transcription factors to modulate gene expression such as collagen production [36]. Furthermore, the translational regulation of the Smads complexes works in concert with other transcription factors such as Snail1, a transcriptional repressor and promoter of EMT [23,33]. We further figured out the underlying mechanisms involved in the EMT process by ISE. ISE administration inhibited EMT of lung fibrosis or TGF-β-treated A549 cells possibly through the decrease of Smad2/3 phosphorylation and the reduction of Snail1 expression, suggesting that ISE's effects on EMT might be due to inhibiting nuclear translocation and binding of Smad2/3 to Snail1 to form a Snail1-Smad2/3 complex. However, whether ISE treatment directly interfere with the formation of the Snail1-Smad2/3 complex needs to be explored.

As far as we know, whether mushroom *I. Sanghuang* and its' extract such as ISE's could affect TGF-β and TGF-β/Smad2/3 signal is unclear. Our result indicates that ISE might be able to affect Smad2/3 activation in vitro directly. However, whether ISE directly regulates Smad2/3 phosphorylation is not known. We hypothesize that ISE impacted Smad2/3 phosphorylation at least in part via an indirect manner *in vivo*, which might be due to the suppression of endogenous TGF-β production by ISE and, subsequently, the reduction of Smad2/3 phosphorylation induced by TGF-β. Current data suggest that ISE inhibits Smad2/3 phosphorylation possibly via a decrease of TGF-β level *in vivo*. However, it is unclear how ISE affects lung fibrosis by directly suppressing Smad2/ 3 phosphorylation or TGF-β-induced Smad2/3 phosphorylation.

The features of EMT are defined as the changes of EMT markers as well as the morphological change. This study aimed to determine the morphological change in TGF-β-treated A549 cells, and ISE administration decreased the number of fibroblast-like or spindle-shaped. Meanwhile, ISE repressed the reduced expression of epithelial marker E-cadherin expression and the increased expression of mesenchymal phenotype markers α-SMA and vimentin in human A549 cells treated by TGF-β *in vitro*.

To exclude the possibility that the inhibitory impact of ISE on the α-SMA expression in A549 cells treated with TGF-β may be due to ISE's cytotoxicity, we performed the CCK8 assay. There was no evidence of

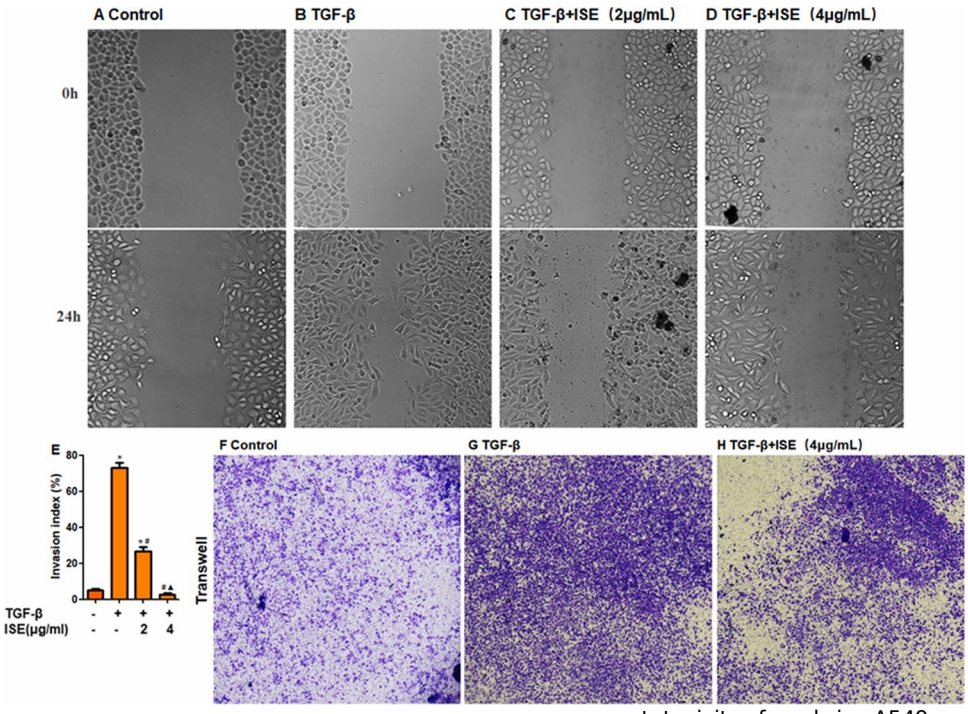

Fig. 8. ISE inhibits the invasion and metastasis of TGF-β-induced the A549 cells. Representative images of the wound area obtained at 0 and 24 h after scratching (magnification, 100×) (A to D), and the invasion index was calculated by formula described as the "*Materials and Methods*" section (E). Values are expressed as the mean ±SEM of three samples. $*p < 0.05$ vs. control; $^{\#}p < 0.05$ vs. TGF-β; $^{\bullet}p < 0.05$ vs TGF- β+ ISE (2μg/mL). Additionally, A549 cells were seeded in the upper transwell chamber and cultured for 24 h. The transmigrating cells were stained with crystal violet and visualized by a microscope (magnification, 100 ×) (F to H).
ISE, *I. sanghuang* polyphenol extract.

cytotoxicity found in A549 cells cultured in the presence of ISE at the indicated concentration. This data allowed us to eliminate ISE's direct cytotoxic effect as a cause for the α-SMA decrease.

EMT is a process of the epithelial cells transforming into a mesenchymal state that involves normal embryonical development and organ fibrosis, tumor migration/invasion [37,38]. In this process, epithelial cells lose epithelial polarity and acquire mesenchymal phenotypes, endowing them with migratory and invasive properties. Thus, it plays a crucial role in protecting against EMT. Currently, we proved that ISE could suppress A549 cell migration and invasion via inhibiting the TGF-β-induced EMT. Importantly, we found that ISE treatment can not result in A549 cell death in the absence of TGF-β. These data suggest that ISE can impair EMT that contributes to reducing fibrosis.

ISE has been proved to have a more prominent influence on the attenuation of acute lung injury in the early stages of BLM-induced mice [21], while continued treatment with ISE had a more significant impact on the inhibition of collagen deposition in mice lung treated with BLM. Thus, we speculate that ISE might prevent IPF progression by reducing the early acute lung injury caused by inflammatory and oxidative stress processes. Furthermore, ISE administration did not significantly affect the change of TGF-β production at an early stage *in vivo* (day 3, date not shown), which was only observed at a later stage. These data suggest that ISE might be able to inhibit the late TGF-β production at the indicated time in this study to implement an anti-fibrotic effect in BLM-treated mice. However, whether ISE affects the TGF-β synthesis or latent TGF-β activation at the other time point needs to be elucidated. Furthermore, it is still unclear whether ISE has a therapeutic effect on pulmonary fibrosis in the BLM-induced lung injury phase.

Polyphenols, the secondary metabolites of mushrooms *Inonotus*, have a wide range of bioactivities such as anti-fibrosis. ISE used in this

study has been identified to contain six polyphenolic compounds: chlorogenic acid, quercetin, quercitrin, rutin, isorhamnetin, and icarisid II and could attenuate acute lung injury at a higher dose (0.6%) through the inhibitory effects of inflammation and oxidative stress. Isorhamnetin has been proved to protect against BLM-induced pulmonary fibrosis via the inhibition of endoplasmic reticulum stress and EMT [39]. Quercetin ameliorated IPF by boosting the anti-oxidant response and suppressing the production of pro-inflammatory cytokines [40,41]. Other compounds, such as chlorogenic acid, reduced BLM-induced pulmonary fibrosis via endoplasmic reticulum stress inhibition [42]. These results indicated that one phenolic compound of ISE could protect against IPF induced by BLM. However, whether the combination of these phenolic compounds could synergistically or additively enhance the anti-fibrosis effect remains to be elucidated. Data from our study demonstrate that amelioration of BLM-induced lung fibrosis by ISE pre-supplementation is possible to be mediated at least in part through *I. sanghuang* polyphenol extract, suggesting the combined impact of the ISE's compounds.

Sex and sex hormones have been shown to contribute to the development of lung fibrosis and lung function decline in BLM-treated mice [43,44]. Male or exogenous androgen-treated mice have an exacerbating role in the deterioration of lung function after BLM treatment; whereas, lung function decline is not influenced by estrogen or female mice. There is no difference in lung fibrosis's commonly measured parameters, including lung cell infiltration, collagen deposition, and lung fibrosis between BLM-induced male and female mice [43]. In contrast, Redente et al. reported that young male mice developed a more fibrotic disease post-instillation with BLM than young female mice, including increased lung collagen deposition (hydroxyproline levels) [44]. However, in another pulmonary fibrotic model, young male mice developed more extensive pulmonary fibrosis; but female mice had more lung inflammatory cells than male mice, not be found in ovariectomized mice after silica-instillation [45]. These findings indicate that sex hormones might have different effects on lung inflammation and fibrosis in various settings. However, this study has a limitation that we only used female mice to demonstrate the impact of ISE on lung fibrosis induced by BLM. Primarily, we should consider the sex importance of experimental groups in lung inflammation and fibrosis studies.

In summary, the present study revealed that ISE from wild *I. sanghuang* inhibited EMT in BLM-induced lung fibrosis. Current findings may offer novel insights into understanding the pathogenesis of IPF, and ISE may be promising as a preventive/therapeutic anti-fibrotic treatment. Further investigations are necessary to clarify the full anti- fibrotic potential therapeutic benefit of ISE or ISE's compounds as concomitant prevention/therapy for patients with IPF with BLM treatment in both *in vivo* and *in vitro* models. Finally, nutritional intervention such as mushroom *I. sanghuang* or its extraction may be used to prevent some chronic disease development such as pulmonary fibrosis.

Author contributions

JW, XS, KL, and YZ contributed to the design of the study. XS, KL, YX, MZ, and XW performed the experiments. XS and KL analyzed the data. XS, KL, YZ, and JW wrote or critically revised the manuscript. All authors read and approved the final manuscript.

Declaration of Competing Interest

The authors report no declarations of interest.

Acknowledgments

This work was supported by the National Natural Science Foundation of China (81402677), the Natural Science Foundation of Henan (202300410080), the Science and Technology Development Project of Henan Province (192102310104, 202102310369), the Science Research Program for Colleges and Universities of Hebei Province (ZD2016074), and the Program of Scientific Research and Cultivation of Young Talents of College of Medicine at Henan University (2019008).

Appendix A. Supplementary data

Supplementary material related to this article can be found, in the online version, at doi:https://doi.org/10.1016/j.biopha.2020.110919.

References

[1] G. Raghu, B. Rochwerg, Y. Zhang, C.A. Garcia, A. Azuma, J. Behr, J.L. Brozek, H. R. Collard, W. Cunningham, S. Homma, T. Johkoh, F.J. Martinez, J. Myers, S. L. Protzko, L. Richeldi, D. Rind, M. Selman, A. Theodore, A.U. Wells, H. Hoogsteden, H.J. Schunemann, S. American Thoracic, s. European Respiratory, S. Japanese Respiratory, A. Latin American Thoracic, An official ATS/ERS/JRS/ ALAT clinical practice guideline: treatment of idiopathic pulmonary fibrosis. An update of the 2011 clinical practice guideline, Am. J. Respir. Crit. Care Med. 192 (2) (2015) e3–19.

[2] P.J. Wolters, H.R. Collard, K.D. Jones, Pathogenesis of idiopathic pulmonary fibrosis, Annu. Rev. Pathol. 9 (2014) 157–179.

[3] L. Richeldi, H.R. Collard, M.G. Jones, Idiopathic pulmonary fibrosis, Lancet 389 (10082) (2017) 1941–1952.

[4] B. Ley, H.R. Collard, T.E. King Jr., Clinical course and prediction of survival in idiopathic pulmonary fibrosis, Am. J. Respir. Crit. Care Med. 183 (4) (2011) 431–440.

[5] D. Warburton, Developmental responses to lung injury: repair or fibrosis, Fibrogenesis Tissue Repair 5 (Suppl. 1) (2012) S2.

[6] D. Warburton, W. Shi, B. Xu, TGF-beta-Smad3 signaling in emphysema and pulmonary fibrosis: an epigenetic aberration of normal development? Am. J. Physiol. Lung Cell Mol. Physiol. 304 (2) (2013) L83–5.

[7] T.A. Wynn, T.R. Ramalingam, Mechanisms of fibrosis: therapeutic translation for fibrotic disease, Nat. Med. 18 (7) (2012) 1028–1040.

[8] C.J. Scotton, R.C. Chambers, Molecular targets in pulmonary fibrosis: the myofibroblast in focus, Chest 132 (4) (2007) 1311–1321.

[9] Y.M. Liu, K. Nepali, J.P. Liou, Idiopathic pulmonary fibrosis: current status, recent progress, and emerging targets, J. Med. Chem. 60 (2) (2017) 527–553.

[10] X. Ma, Y. Zhang, D. Jiang, Y. Yang, G. Wu, Z. Wu, Protective effects of functional amino acids on apoptosis, inflammatory response, and pulmonary fibrosis in lipopolysaccharide-challenged mice, J. Agric. Food Chem. 67 (17) (2019) 4915–4922.

[11] C.-Y. Chen, W.-H. Peng, L.-C. Wu, C.-C. Wu, S.-L. Hsu, Luteolin ameliorates experimental lung fibrosis both in vivo and in vitro: implications for therapy of lung fibrosis, J. Agric. Food Chem. 58 (22) (2010) 11653–11661.
[12] N. Yahfoufi, N. Alsadi, M. Jambi, C. Matar, The immunomodulatory and anti- inflammatory role of polyphenols, Nutrients 10 (11) (2018).
[13] J.G. Han, M.W. Hyun, C.S. Kim, J.W. Jo, J.H. Cho, K.H. Lee, W.S. Kong, S.K. Han, J. Oh, G.H. Sung, Species identity of Phellinus linteus (sanghuang) extensively used as a medicinal mushroom in Korea, J. Microbiol. 54 (4) (2016) 290–295.
[14] J.Y. Jung, I.K. Lee, S.J. Seok, H.J. Lee, Y.H. Kim, B.S. Yun, Antioxidant polyphenols from the mycelial culture of the medicinal fungi Inonotus xeranticus and Phellinus linteus, J. Appl. Microbiol. 104 (6) (2008) 1824–1832.
[15] H. Chen, T. Tian, H. Miao, Y.Y. Zhao, Traditional uses, fermentation, phytochemistry and pharmacology of Phellinus linteus: a review, Fitoterapia 113 (2016) 6–26.
[16] M. Song, H.-J. Park, Anti-inflammatory effect of Phellinus linteus grown on germinated brown rice on dextran sodium sulfate-induced acute colitis in mice and LPS-activated macrophages, J. Ethnopharmacol. 154 (2) (2014) 311–318.
[17] S.B. Han, C.W. Lee, Y.J. Jeon, N.D. Hong, I.D. Yoo, K.H. Yang, H.M. Kim, The inhibitory effect of polysaccharides isolated from Phellinus linteus on tumor growth and metastasis, Immunopharmacology 41 (2) (1999) 157–164.
[18] X.M. Tian, Y.C. Dai, A.R. Song, K. Xu, L.T. Ng, Optimization of liquid fermentation medium for production of inonotus sanghuang (Higher Basidiomycetes) mycelia and evaluation of their mycochemical contents and antioxidant activities, Int. J. Med. Mushrooms 17 (7) (2015) 681–691.
[19] K. Liu, X. Xiao, J. Wang, C.Y.O. Chen, H. Hu, Polyphenolic composition and antioxidant, antiproliferative, and antimicrobial activities of mushroom Inonotus sanghuang, LWT - Food Sci. Technol. 82 (2017) 154–161.
[20] M. Zhang, Y. Xie, X. Su, K. Liu, Y. Zhang, W. Pang, J. Wang, Inonotus sanghuang polyphenols attenuate inflammatory response via modulating the crosstalk between macrophages and adipocytes, Front. Immunol. 10 (2019) 286.
[21] X. Su, K. Liu, Y. Xie, M. Zhang, Y. Wang, M. Zhao, Y. Guo, Y. Zhang, J. Wang, Protective effect of a polyphenols-rich extract from Inonotus Sanghuang on bleomycin-induced acute lung injury in mice, Life Sci. 230 (2019) 208–217.
[22] T. Ashcroft, J.M. Simpson, V. Timbrell, Simple method of estimating severity of pulmonary fibrosis on a numerical scale, J. Clin. Pathol. 41 (4) (1988) 467–470.
[23] T. Vincent, E.P. Neve, J.R. Johnson, A. Kukalev, F. Rojo, J. Albanell, K. Pietras, H. Virtanen, L. Philipson, P.L. Leopold, R.G. Crystal, A.G. de Herreros, A. Moustakas, R.F. Pettersson, J. Fuxe, A SNAIL1-SMAD3/4 transcriptional repressor complex promotes TGF-beta mediated epithelial-mesenchymal transition, Nat. Cell Biol. 11 (8) (2009) 943–950.
[24] S. Lamouille, J. Xu, R. Derynck, Molecular mechanisms of epithelial-mesenchymal transition, Nat. Rev. Mol. Cell Biol. 15 (3) (2014) 178–196.
[25] Y. Aschner, G.P. Downey, Transforming growth factor-beta: master regulator of the respiratory system in health and disease, Am. J. Respir. Cell Mol. Biol. 54 (5) (2016) 647–655.
[26] D.G. Hoyt, J.S. Lazo, Alterations in pulmonary mRNA encoding procollagens, fibronectin and transforming growth factor-beta precede bleomycin-induced pulmonary fibrosis in mice, J. Pharmacol. Exp. Ther. 246 (2) (1988) 765–771.
[27] I.G. Luzina, N.W. Todd, S. Sundararajan, S.P. Atamas, The cytokines of pulmonary fibrosis: much learned, much more to learn, Cytokine 74 (1) (2015) 88–100.
[28] A. Bergeron, P. Soler, M. Kambouchner, P. Loiseau, B. Milleron, D. Valeyre, A. H. Hance, A. Tazi, Cytokine profiles in idiopathic pulmonary fibrosis suggest an important role for TGF-β and IL-10, Eur. Respir. J. 22 (1) (2003) 69–76.
[29] N. Khalil, R.N. O'Connor, H.W. Unruh, P.W. Warren, K.C. Flanders, A. Kemp, O. H. Bereznay, A.H. Greenberg, Increased production and immunohistochemical localization of transforming growth factor-beta in idiopathic pulmonary fibrosis, Am. J. Respir. Cell Mol. Biol. 5 (2) (1991) 155–162.
[30] N. Kaminski, J.D. Allard, J.F. Pittet, F. Zuo, M.J. Griffiths, D. Morris, X. Huang, D. Sheppard, R.A. Heller, Global analysis of gene expression in pulmonary fibrosis reveals distinct programs regulating lung inflammation and fibrosis, Proc. Natl. Acad. Sci. U. S. A. 97 (4) (2000) 1778–1783.
[31] G. Mignot, H. Bugaut, F. Ghiringhelli, Immune ambivalence, OncoImmunology 2 (9) (2013) e25737.
[32] A.L. Tatler, G. Jenkins, TGF-β activation and lung fibrosis, Proc. Am. Thorac. Soc. 9 (3) (2012) 130–136.
[33] M. Trojanowska, Noncanonical transforming growth factor beta signaling in scleroderma fibrosis, Curr. Opin. Rheumatol. 21 (6) (2009) 623–629.
[34] S. Nakerakanti, M. Trojanowska, The role of TGF-beta receptors in fibrosis, Open Rheumatol. J. 6 (2012) 156–162.
[35] B.M. Chacko, B.Y. Qin, A. Tiwari, G. Shi, S. Lam, L.J. Hayward, M. De Caestecker, K. Lin, Structural basis of heteromeric smad protein assembly in TGF-beta signaling, Mol. Cell 15 (5) (2004) 813–823.
[36] L. DeMaio, S.T. Buckley, M.S. Krishnaveni, P. Flodby, M. Dubourd, A. Banfalvi, Y. Xing, C. Ehrhardt, P. Minoo, B. Zhou, E.D. Crandall, Z. Borok, Ligand- independent transforming growth factor-β type I receptor signalling mediates type I collagen-induced epithelial–mesenchymal transition, J. Pathol. 226 (4) (2012) 633–644.
[37] M. Diepenbruck, G. Christofori, Epithelial-mesenchymal transition (EMT) and metastasis: yes, no, maybe? Curr. Opin. Cell Biol. 43 (2016) 7–13.
[38] I. Pastushenko, C. Blanpain, EMT transition states during tumor progression and metastasis, Trends Cell Biol. 29 (3) (2019) 212–226.
[39] Q. Zheng, M. Tong, B. Ou, C. Liu, C. Hu, Y. Yang, Isorhamnetin protects against bleomycin-induced pulmonary fibrosis by inhibiting endoplasmic reticulum stress and epithelial-mesenchymal transition, Int. J. Mol. Med. 43 (1) (2019) 117–126. [40] D. Impellizzeri, E. Talero, R. Siracusa, A. Alcaide, M. Cordaro, J. Maria Zubelia, G. Bruschetta, R. Crupi, E. Esposito, S. Cuzzocrea, V. Motilva, Protective effect of polyphenols in an inflammatory process associated with experimental pulmonary fibrosis in mice, Br. J. Nutr. 114 (6) (2015) 853–865.
[41] C. Veith, M. Drent, A. Bast, F.J. van Schooten, A.W. Boots, The disturbed redox- balance in pulmonary fibrosis is modulated by the plant flavonoid quercetin, Toxicol. Appl. Pharmacol. 336 (2017) 40–48.
[42] Y.C. Wang, J. Dong, J. Nie, J.X. Zhu, H. Wang, Q. Chen, J.Y. Chen, J.M. Xia, W. Shuai, Amelioration of bleomycin-induced pulmonary fibrosis by chlorogenic acid through endoplasmic reticulum stress inhibition, Apoptosis 22 (9) (2017) 1147–1156.
[43] J.W. Voltz, J.W. Card, M.A. Carey, L.M. Degraff, C.D. Ferguson, G.P. Flake, J. C. Bonner, K.S. Korach, D.C. Zeldin, Male sex hormones exacerbate lung function impairment after bleomycin-induced pulmonary fibrosis, Am. J. Respir. Cell Mol. Biol. 39 (1) (2008) 45–52.
[44] E.F. Redente, K.M. Jacobsen, J.J. Solomon, A.R. Lara, S. Faubel, R.C. Keith, P. M. Henson, G.P. Downey, D.W.H. Riches, Age and sex dimorphisms contribute to the severity of bleomycin-induced lung injury and fibrosis, Am. J. Physiol.-Lung Cell. Mol. Physiol. 301 (4) (2011) L510–L518.
[45] D.M. Brass, S.P. McGee, M.K. Dunkel, S.M. Reilly, J.M. Tobolewski, T. Sabo-Attwood, C.L. Fattman, Gender influences the response to experimental silica-induced lung fibrosis in mice, Am. J. Physiol.-Lung Cell. Mol. Physiol. 299 (5) (2010) L664–L671.